

Heat Capacities and Thermodynamic Properties of the Iron Selenides $\text{Fe}_{1.04}\text{Se}$, Fe_7Se_8 , and Fe_3Se_4 from 298 to 1050°K

FREDRIK GRØNVOLD

Kjemisk Institutt A, Universitetet i Oslo, Blindern, Oslo 3, Norway

Heat capacities of the iron selenides $\text{Fe}_{1.04}\text{Se}$, Fe_7Se_8 , and Fe_3Se_4 have been measured by adiabatic shield calorimetry in the range 298 to 1050°K. At high temperatures they all have the Fe_{1-x}Se -phase with NiAs-like structure as main or sole constituent. In $\text{Fe}_{1.04}\text{Se}$ a first order peritectoid transition from tetragonal (PbO-type) to hexagonal (NiAs-type) structure and surplus iron is observed at 730.8°K with an entropy increment of $6.690 \text{ J } ^\circ\text{K}^{-1}$ per 1/2.04 mole $\text{Fe}_{1.04}\text{Se}$. The entropy and enthalpy increments, $(X_{1000}^\circ - X_{298}^\circ)$ including those of the transition, are $44.63 \text{ J } ^\circ\text{K}^{-1}$ and $28\,080 \text{ J}$ per 1/2.04 mole $\text{Fe}_{1.04}\text{Se}$, respectively. The high heat capacity values of $\text{Fe}_{1.04}\text{Se}$ below the transition are indicative of a non-cooperative process involving 1 and 4 spin states taking place in the sample. Fe_7Se_8 shows two λ -type transitions, one with maximum heat capacity at 451°K associated with a transition from ferri- to paramagnetism in the sample, and one with maximum at 638°K connected with a structural change in the sample. A tentative separation of the first transition from the background results in an entropy increment of $13.0 \text{ J } ^\circ\text{K}^{-1}$ per mole of iron atoms, which is in reasonable agreement with the calculated spin disorder entropies of Fe(II) and Fe(III). The entropy increment of the second transition, $2.5 \text{ J } ^\circ\text{K}^{-1}$ per 0.875 mole of iron atoms, is close to the expected value for disorder in the partly filled layers of iron atoms. The total entropy and enthalpy increments between 298.15 and 1000°K are $39.84 \text{ J } ^\circ\text{K}^{-1}$ and $22\,980 \text{ J}$ per 1/15 mole Fe_7Se_8 . Fe_3Se_4 shows a λ -type transition with maximum at 977°K in addition to the earlier known transition at 307°K. A reevaluation of the entropy increment of the latter transition supports the view of a ferri- to paramagnetic transition with only two spin states per iron atom, followed by a non-cooperative transition probably involving 3 additional spin states for Fe(II) and 4 for Fe(III). The 977°K transition is apparently of a structural nature, involving the disorder of vacancies within the half-filled iron layers. The associated entropy increment is estimated to be $3.5 \text{ J } ^\circ\text{K}^{-1}$ per 0.75 mole of iron atoms. The total entropy and enthalpy increments between 298.15 and 1000°K are $30.61 \text{ J } ^\circ\text{K}^{-1}$ and $24\,000 \text{ J}$ per 1/7 mole Fe_3Se_4 .

A thermophysical study of the iron selenides is of special interest in connection with the structural and magnetic properties in the Fe_{1-x}Se phase region. In this region structures of NiAs-like type occur with various kinds of vacancy distribution. Low temperature heat capacities in the range 5 to 350°K have been reported for three intermediate compounds and extensive references to earlier work on the iron selenium system have been given.¹

In the present study heat capacities for substances with the same three compositions have been measured from room temperature to about 1050°K and several maxima in heat capacity were found to be present. For iron monoselenide a structural change from tetragonal PbO-type to hexagonal NiAs-type is known to take place in the temperature range 300 to 500°C. This change is probably not a strict polymorphism, but involves phases of different compositions. The low-temperature phase with PbO-type structure has the approximate composition $\text{Fe}_{1.04}\text{Se}$, while the NiAs-type high-temperature phase in equilibrium with it has close to stoichiometric composition. Above the transition temperature the sample consists of a mixture of the Fe_{1-x}Se -phase and small amounts of iron. A sample with composition $\text{Fe}_{1.04}\text{Se}$ was therefore prepared and its heat capacity and enthalpy of transition measured. The two other samples studied have compositions Fe_7Se_8 and Fe_3Se_4 , respectively. At elevated temperatures they represent the Fe_{1-x}Se -phase with NiAs-like structure and vacant metal sites which become ordered on cooling and give rise to superstructures and also to ferrimagnetism.

While the heat capacity behaviour associated with the disappearance of ferrimagnetism in Fe_3Se_4 around 35°C has been measured accurately,¹ and that of Fe_7Se_8 qualitatively,² the behaviour associated with the structural changes has not yet been clarified. Thus, Hirone and Chiba² attributed the heat effect at 350°C to a eutectoid reaction



The structural changes taking place in Fe_7Se_8 on heating have been studied by X-rays by Okazaki and Hirakawa³ and in more detail by Okazaki.^{4,5} For slowly cooled samples a triclinic superstructure of NiAs-like type with ordered vacancies and quadrupled C -axis, $C = 4c$, was observed. Quenching from 320°C resulted in another superstructure with $C = 3c$. The ordering scheme of the vacancies in every other plane perpendicular to the c -axis has been confirmed in the neutron diffraction work by Andresen and Leciejewicz,⁶ on a sample which showed the $3c$ -structure after slow cooling from 600°C.

Okazaki found the transition from the $4c$ - to the $3c$ -structure to be independent of the ferri- to paramagnetic transition and to take place gradually with the two structures coexisting in the temperature range 240 to 298°C. It was not completely reversible. In the temperature range 360 to 375°C a similar gradual transition from the $3c$ -structure to a partially disordered state was found to take place. During the transition the vacancies remained within alternate planes, but became distributed at random over positions in these planes on heating. At about 400°C the vacancies were assumed to become completely disordered. For some specimens an intermediate structure between the $3c$ - and the disordered structure was found to develop in the range 320 to 385°C and to disappear around 450°C. Thus, for Fe_7Se_8 a considerable number

of transitions were to be expected, even though some of the structures reported by Okazaki might be attributed to variations in composition of the samples, perhaps also as a result of oxidation.

In case of Fe_3Se_4 the X-ray work by Okazaki and Hirakawa³ showed a doubling of the c -axis of the monoclinic unit cell by Hägg and Kindström⁷ and that the vacancies were ordered in every other metal layer parallel to the ab -plane. No data have been presented, however, about the disappearance of the ordered distribution on the vacancies and the associated structural changes.

In the present work it was further thought of interest to attempt separations of the magnetic and structural order-disorder contributions from the heat capacity of the compounds and to compare them with calculated values for simplified models of the changes involved.

EXPERIMENTAL

A. Samples. All three samples were synthesized from high-purity iron and selenium. "Ferrum reductum pro analysi" from E. Merck was reduced with dry, purified hydrogen gas at 1000°C until constant weight was attained. A spectrographic analysis showed the presence of about 0.01 % Ni and Si and about 0.001 % Mn. The high-purity selenium was a gift from Bolidens Gruvaktiebolag and contained according to their analyses these impurities (in ppm): Cl (2), Fe (0.8), K (0.3), Na (0.4), non-volatile matter (12). The following elements were not detected (the numbers indicate sensitivity limits in ppm): Ag (0.03), Al (0.3), As (1), Bi (0.1), Ca (1), Cr (0.3), Cu (0.1), Hg (0.5), Mg (0.3), Mn (0.1), Ni (0.3), Pb (0.3), S (5), Sb (1), Si (1), Sn (0.3), Te (1), Zn (1).

Accurately weighed quantities corresponding to the above compositions were heated in evacuated and sealed quartz tubes. Because of the transitions in the solid selenides, which sometimes cause cracking of the sample tubes on cooling, the tubes were put into larger quartz tubes which were also evacuated and sealed. The samples were fused for 4 h at 1050°C in an electric muffle furnace, cooled to room temperature and fragmented under dry nitrogen in an agate mortar. They were then homogenized at 350°C for 30 days and cooled to room temperature over another 30 days.

Transfer of the samples to the quartz ampoules for heat capacity measurements was also carried out under dry nitrogen gas. The mass of samples used was 135.838 g $\text{Fe}_{1.04}\text{Se}$, 171.592 g Fe_2Se_3 and 131.171 g Fe_3Se_4 .

B. Calorimetric apparatus. Measurements were made in an adiabatic shield type calorimeter previously described,⁸ with intermittent energy input and temperature equilibration between each input. The quartz ampoules containing the samples have a central well for the heater and platinum resistance thermometer. They are inserted in the silver calorimeter, and the whole assembly is surrounded by three silver shields with enclosed heaters. The calorimeter and the shield systems are encompassed by a guard heater system of silver and placed in a vertical tube furnace.

The temperature differences between corresponding parts of calorimeter and shields are measured by means of Pt 90%Pt10%Rh thermopiles. The amplified signals are recorded and simultaneously used for automatically controlling the energy input to the shield heaters to maintain quasiadiabatic conditions during input and drift periods. The temperature of the three guard bodies is kept automatically 0.4°C below the shield temperature, and that of the furnace windings 10°C lower.

The heat capacity of the container-calorimeter-heater-thermometer assembly was determined in a separate series of experiments. Small corrections were applied for the differences in mass of the quartz containers, for temperature excursions of the shields from the calorimeter temperature, for "zero" drift of the calorimeter, and for curvature. All measurements of temperature, resistance and potential are based upon calibrations or standardizations by the U.S. National Bureau of Standards.

C. X-Ray examination. Room temperature lattice constant data were obtained in Guinier-type focusing cameras using $\text{CuK}\alpha_1$ -radiation ($\lambda = 1.54051 \text{ \AA}$) with potassium

Table 1. Heat capacities of iron selenides, joule mole⁻¹ °K⁻¹.

<i>T</i> , °K	<i>C_p</i>	<i>T</i> , °K	<i>C_p</i>
1/2.04 Fe _{1.04} Se (1 mole Fe _{0.510} Se _{0.490} = 67.17 g)			
Series I		510.59	32.15
689.72	34.09	522.32	32.36
701.19	34.79	533.96	32.64
712.48	34.82	545.53	32.81
729.79	35.42	557.97	33.01
		571.29	33.20
		584.52	33.36
Series II Δ <i>H</i> -run		597.67	33.54
727.54)	4934.0 *	610.76	33.44
736.39)		623.78	33.72
Series III		Series VI	
915.44	31.19	625.01	33.64
928.06	31.76	638.42	33.82
940.54	32.22	651.59	34.02
952.83	33.08	664.68	34.16
964.99	33.10	677.70	34.32
977.16	33.13	690.63	34.57
990.22	33.75	703.52	34.52
1004.13	34.50	715.42	34.94
1017.72	34.92	723.60	35.27
1031.41	35.42	727.34	35.55
1044.89	35.31	729.54	35.71
New calorimeter Series IV		Series VII Δ <i>H</i> -run	
307.84	28.15	730.72)	4899.3 *
322.35	28.58	730.90)	
335.43	28.93	Series VIII	
348.32	29.18	750.82	29.93
361.05	29.50	763.05	29.83
373.60	29.86	776.23	29.67
386.00	30.14	789.42	29.70
398.18	30.35	802.58	29.71
410.22	30.58	815.74	29.74
422.24	30.74	828.81	29.90
		841.84	29.98
Series V		854.80	30.17
450.72	31.42	867.70	30.33
462.86	31.43	880.53	30.70
474.91	31.62	894.15	31.21
486.89	31.88	908.60	31.27
498.78	32.03	922.88	32.63

* Enthalpy increment, joule mole⁻¹, over the temperature interval indicated.

Table 1. Continued.

T , °K	C_p	T , °K	C_p
1/15 Fe ₇ Se ₈ (1 mole Fe _{0.467} Se _{0.533} = 68.18 g)			
Series I		Series IV	
302.76	29.70	583.52	31.97
317.83	30.33	594.15	32.79
332.52	30.97	604.57	34.06
347.82	31.74	612.22	35.37
360.75	32.37	622.09	38.52
370.62	32.99	626.71	42.76
376.55	33.27	631.06	46.37
382.24	33.65	635.20	51.52
389.64	34.22	639.08	57.68
398.66	34.82	642.83	56.26
408.00	35.60	646.91	45.19
417.17	36.50	651.68	34.78
426.15	37.75	656.93	31.71
434.87	39.09	664.86	31.31
443.34	41.15		
451.57	42.14		
420.26	34.27		
Series II		Series V	
434.15	38.88	620.74	36.64
439.36	40.10	625.50	40.06
444.43	41.53	629.51	47.10
448.35	42.53	633.90	54.99
451.15	42.98	636.72	57.81
453.97	41.34	638.56	57.94
456.69	36.11	642.59	52.09
460.07	34.10	644.57	49.20
463.26	33.38	646.65	43.62
466.48	32.67	648.94	37.97
469.70	32.38	651.45	32.95
475.89	32.07	655.38	31.79
485.18	31.32	660.67	31.31
494.64	31.03	665.89	31.00
Series III		Series VI	
476.55	31.93	675.84	31.30
483.99	31.39	687.32	31.12
493.34	31.06	699.72	30.90
503.59	30.87	712.19	30.97
514.74	30.85	724.64	30.85
525.83	30.87	737.08	30.73
536.87	30.99	749.53	30.70
547.85	31.20	761.95	30.60
558.72	31.37	774.36	30.58
569.54	31.71	786.76	30.69
580.27	32.08	799.14	30.72
590.90	32.83	811.51	30.84
		823.85	30.81

Table 1. Continued.

T , °K	C_p	T , °K	C_p
Series VII		New calorimeter	
826.59	30.76	Series X	
840.30	30.91	673.42	31.08
854.85	31.02	686.22	30.82
869.35	31.29	699.87	30.67
883.78	31.46	713.53	30.56
Series VIII		Series XI	
786.38	30.61	716.09	30.47
797.22	30.37	729.64	30.49
808.02	30.62	720.06	30.39
819.23	30.69	733.54	30.52
830.39	30.74	746.98	30.48
841.51	30.87	Series XII	
852.62	30.80	665.87	31.10
863.71	30.93	677.73	31.07
874.75	30.97	691.26	30.93
885.76	31.03	704.79	30.76
896.71	31.22	718.30	30.70
Series IX		731.79	30.64
879.99	31.20	745.25	30.64
891.77	31.05	758.70	30.63
904.44	31.15	772.11	30.71
917.05	31.40	785.50	30.64
930.49	31.54	798.86	30.77
944.76	31.72	812.19	30.62
958.98	31.93	825.48	30.79
973.14	31.99	838.73	30.87
987.26	32.10	851.94	30.89
1001.32	32.83		
1015.43	32.61		
1029.37	32.61		
T , °K	C_p	T , °K	C_p
$\frac{1}{7} \text{Fe}_3\text{Se}_4$ (1 mole $\text{Fe}_{0.429}\text{Se}_{0.571} = 69.06 \text{ g}$)			
Series I		Series II	
303.54	31.31	477.57	29.79
319.65	29.00	491.68	29.90
335.95	28.77	505.62	30.12
352.03	28.80	519.45	30.13
367.79	28.99	533.15	30.23
383.31	29.11	546.74	30.37
398.62	29.38	560.21	30.38
413.71	29.51	573.60	30.45
428.62	29.63	586.91	30.48
443.13	29.71	600.11	30.69
457.48	29.79	613.23	30.90
471.88	29.84	626.26	30.94

Table 1. Continued.

T , °K	C_p	T , °K	C_p
	Series III	1037.28	38.80
605.38	30.99	1051.31	39.08
618.40	30.63		
631.32	30.87		
644.14	31.11		
656.87	31.12		
669.51	31.30		
682.07	31.49		
694.54	31.78		
	Series IV		Series VII
697.78	32.29	702.24	32.15
711.35	32.22	714.88	32.13
723.92	32.24	727.58	32.35
736.41	32.55	740.22	32.68
749.79	32.74	752.81	32.73
763.10	33.26	765.36	33.03
776.37	33.57	777.87	33.22
789.58	33.89	790.31	33.68
802.64	34.13	802.70	33.99
		815.01	34.35
		827.24	34.81
		839.37	35.45
		851.39	35.94
		863.32	36.32
		875.17	36.69
	Series V		Series VIII
817.06	34.75	871.40	36.65
829.71	34.94	883.95	37.22
842.28	35.69	896.28	37.96
854.78	35.81	908.43	39.35
867.20	36.57	920.38	40.57
879.49	37.50	932.13	42.00
891.65	38.50	943.63	44.29
903.65	39.10	954.74	47.89
915.50	40.47	965.11	57.37
927.14	42.00	971.57	95.95
		974.59	99.96
		977.50	107.15
		979.70	89.46
	Series VI	982.00	49.47
920.43	41.20	984.82	37.75
932.58	42.98	989.12	37.59
944.37	45.32	998.14	37.53
955.76	49.25		
966.12	64.37		
972.97	98.47		
977.05	106.46		
982.33	46.10		
989.21	37.24		
999.09	37.29		
1011.64	37.13		
1024.07	38.98		
			Series IX
		1009.25	36.92
		1022.03	37.65
		1035.56	38.01
		1048.98	38.24
		1059.82	38.64

chloride ($a_{20} = 6.2919 \text{ \AA}$ according to Hambling⁹) as a calibrating substance. High temperature X-ray photographs were taken in a 19 cm diameter Unicam camera with iron radiation ($\lambda\text{FeK}\alpha_1 = 1.93597 \text{ \AA}$). The samples were sealed in thin-walled quartz capillaries. By means of a voltage regulator the temperature was kept constant within $\pm 3^\circ\text{C}$ during an exposure. The Pt-PtRh thermocouples of the furnace were calibrated with a standard couple located at the position of the specimen, and the temperatures given probably represent the sample temperatures within $\pm 5^\circ\text{C}$. The estimated standard deviations in the lattice constant values are less than 0.05 %.

RESULTS

Results of the heat-capacity determinations are listed in Table 1 in chronological order. The data are expressed in terms of one mole of mixture, $\text{Fe}_x\text{Se}_{1-x}$, *i.e.* 67.17 g $\text{Fe}_{1.04}\text{Se}$, 68.18 g Fe_7Se_8 , and 69.06 g Fe_3Se_4 taking the atomic weights of iron and selenium to be 55.85 and 78.96, respectively. The approximate temperature increments can usually be inferred from the adjacent mean temperatures in Table 1. In case with Fe_3Se_4 a slight decomposition of the sample takes place at the highest temperatures and an evaporation correction had to be applied on basis of the selenium pressures measured by Svendsen¹⁰ using the method described by Hoge.¹¹ The corrections increased from a negligible value at 900°K to 0.7 % at 1060°K .

The heat-capacity *versus* temperature curves are shown in Fig. 1 for $\text{Fe}_{1.04}\text{Se}$ and Fe_7Se_8 , and in Fig. 2 for Fe_3Se_4 . The heat capacity of $\text{Fe}_{1.04}\text{Se}$

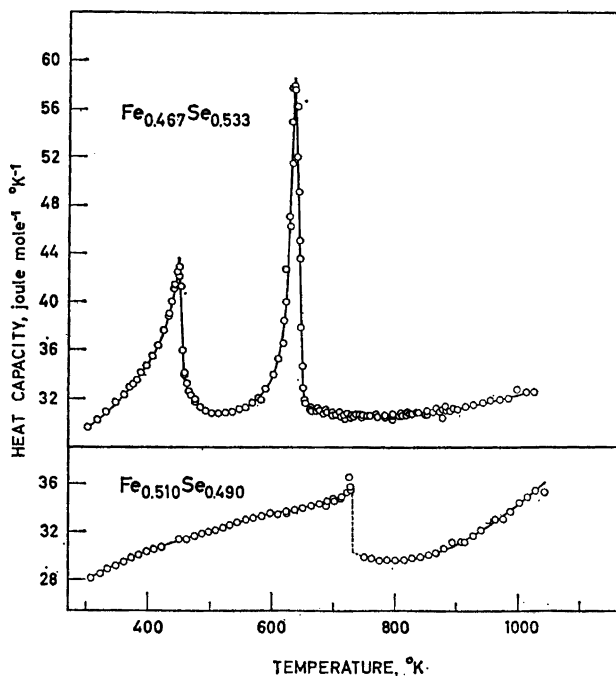


Fig. 1. Heat capacities of 1/2.04 mole $\text{Fe}_{1.04}\text{Se}$ and 1/15 mole Fe_7Se_8 as functions of temperature.

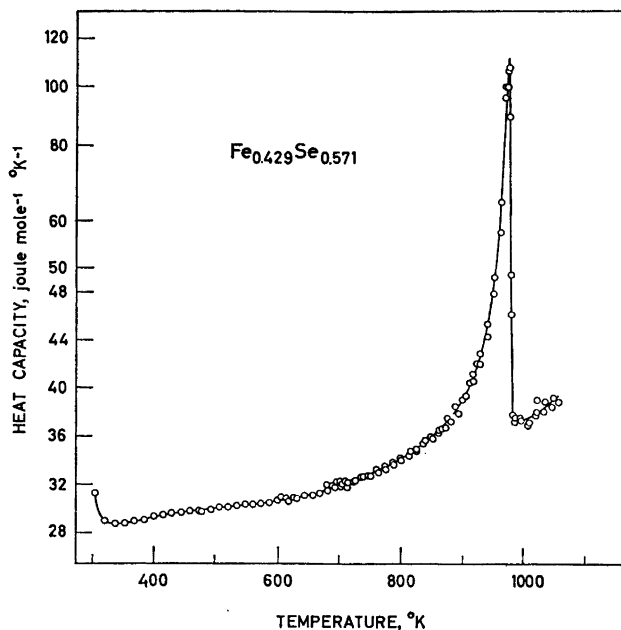


Fig. 2. Heat capacity of 1/7 mole Fe₃Se₄ as a function of temperature. Note logarithmic scale above 50 joule mole⁻¹ °K⁻¹.

increases regularly up to about 730°K, where a phase transformation occurs. The high-temperature product has considerably lower heat capacity than the low-temperature phase, with values rather similar to those observed for Fe₇Se₈.

The transformation in Fe_{1.04}Se was noted after the fourth energy input of Series I (see Table 1) in form of a slightly negative drift in the calorimeter temperature. The next energy input resulted in a slow approach to equilibrium, this time to a temperature lower than before the input. The measurements were discontinued and the sample allowed to cool to about 700°K overnight, in order that it might revert to its low-temperature state. Successive energy inputs were then applied, see Table 2, and the limiting temperature after each input calculated according to the Reshetnikov equation¹²

$$R_t = \frac{R_0 + At}{1 + Bt}$$

In this equation R_t is the resistance thermometer reading at time t , R_0 the reading at time zero, while A and B are constants. The limiting temperature at which the phase transition ceases is given by the ratio $A/B = R_\infty$. The equation assumes a homogeneous reaction. In the present case the equation was used only to get an indication when sufficient energy had been supplied to the system to complete the transformation, without waiting for equilibrium after each energy input. As seen from Table 2, inputs 2 to 10 have approximately the same limiting temperature, while for input 11 the limiting temperature is about 4°K higher, indicating that the transition is completed.

Table 2. Determination of the completion of transformation in $\text{Fe}_{1.04}\text{Se}$ using the Reshetnikov equation for finding the limiting temperature after each energy input.

Input	time, min	joule	T_{∞} , °K
1	0	2041.73	727.54
2	181	2888.81	732.2
3	284	865.38	733.4
4	349	864.24	731.7
5	409	863.37	731.9
6	469	862.20	732.0
7	559	859.94	732.2
8	619	858.49	733.0
9	679	857.47	732.7
10	739	858.01	732.8
11	795	855.03	736.39

The enthalpy and entropy of transformation were then calculated assuming linear approach of the heat capacities to the transformation temperature both for the low- and the high-temperature phases. Any additional pre- and post-transition effects are thus included in the enthalpy of transformation. The values are listed in Table 3, together with results of another series of experiments, Series VIII, in which the transformation temperature was located at $730.8 \pm 0.1^\circ\text{K}$. The mean values are: $\Delta H^{\text{tr}} = 4889 \pm 5 \text{ J mole}^{-1}$ and $\Delta S^{\text{tr}} = 6.690 \pm 0.007 \text{ J mole}^{-1} \text{ }^\circ\text{K}^{-1}$ for $1/2.04 \text{ mole Fe}_{1.04}\text{Se}$. For the same transformation Hirone and Chiba² found $\Delta H = 1575 \text{ J per } 1/2 \text{ mole FeSe}$. The large discrepancy is indicative of the difficulties in calibrating a thermal analysis apparatus.

Table 3. Enthalpy and entropy of transformation of the tetragonal iron monoselenide into the hexagonal: $0.49 \text{ Fe}_{1.04}\text{Se (tet)} = 0.49 \text{ FeSe (hex)} + 0.02 \text{ Fe}$. Units: Joule, $^\circ\text{K}$, mole.

Series	ΔH^{tr}	ΔS^{tr}
II	4884.0	6.683
VIII	4893.5	6.696
Mean value	4889 ± 5	6.690 ± 0.007

In Fe_7Se_8 two lambda-type transitions are noted, see Fig. 1, one with maximum at 451°K and the other with maximum at 638°K . The first one is obviously connected with the disappearance of ferrimagnetism in Fe_7Se_8 , which takes place at about 150°C according to the magnetic measurements by Hirone, Maeda and Tsuya,¹³ at 174°C for $\text{FeSe}_{1.13}$ according to the thermal analysis data by Hirone and Chiba,² and at 210°C according to the neutron

diffraction work by Andresen and Leciejewicz.⁶ The second transition, which is considerably sharper, is apparently connected with one of the order-disorder phenomena found in the X-ray work by Okazaki.⁵ No further anomalies or irregularities in heat capacity were observed in the temperature range up to 1037°K.

The heat-capacity behaviour of Fe₃Se₄ is shown in Fig. 2. From a maximum around 305°K the heat capacity decreases slightly up to 335°K (for details, see Ref. 1) and increases regularly up to 700°K. With further increase in temperature a lambda-type transition develops with a maximum at 978°K. The non-transitional heat capacity also rises in this temperature region and exceeds the Dulong-Petit value quite considerably, *vide infra*.

Values of the thermodynamic properties for the three samples have been calculated using graphically interpolated values of heat capacity. The entropy and enthalpy increments were computed by numerical integration and the values of $S^\circ - S_0^\circ$ and $(H^\circ - H_0^\circ)/T$ are listed in Table 4 for several temperatures after incorporating the previously determined values¹ of $S_{298}^\circ - S_0^\circ$ and $(H_{298}^\circ - H_0^\circ)/T$.

The estimated standard deviation of the individual heat capacity values from the smoothed curve is 0.51 % for Fe_{1.04}Se. It is 0.51 % for Fe₇Se₈, excluding 9 measurements deviating more than 2 % from the curve, and 0.56 % for Fe₃Se₄ excluding 4 such measurements. The values of entropy and enthalpy are considered to be accurate to ± 0.3 %, but additional digits are given because of their importance on a relative scale.

Gibbs energy values are not listed because of the uncertainty as to the presence of complete structural and magnetic order in these samples below 5°K.

DISCUSSION AND SUPPLEMENTARY X-RAY DATA

On comparing the general heat-capacity behavior of the three samples and disregarding the transitions, it appears that the values for Fe_{1.04}Se are rather high in the region from room temperature and up to the transformation temperature of 730.8°K. Another feature is that the heat capacities of Fe_{1.04}Se and of Fe₃Se₄ rise rather sharply at the highest temperatures compared to those of Fe₇Se₈. In addition the energetics of the different transitions needs further consideration.

A. Fe_{1.04}Se. Fe_{1.04}Se has a structure of PbO-like type,^{7,14} with surplus iron atoms in interstitial positions, probably $\frac{1}{2}, 0, z$ and $0, \frac{1}{2}, \bar{z}$ with $z \approx 0.70$. There is no crystallographic evidence that these atoms are ordered under the experimental conditions of this study. Thus, the compound is expected to have zero-point entropy, in the zeroth approximation $S_0^\circ = R (0.96 \ln 0.96 + 0.04 \ln 0.04) = 0.75 \text{ J mole}^{-1} \text{ }^\circ\text{K}^{-1}$.

The magnetic properties of the tetragonal Fe_{1.04}Se-phase have not been studied in detail, but on the basis of results by Hirone *et al.*¹³ for more selenium-rich selenides almost zero magnetization, *i.e.* paramagnetism or antiferromagnetism, is expected for Fe_{1.04}Se. In such a magnetically concentrated compound the magnetic ordering is generally expected to take place at a comparatively high temperature and in a cooperative way. Since no λ -type

Table 4. Thermodynamic properties of iron selenides, joule mole⁻¹ °K⁻¹.

T, °K	1/2.042 Fe _{1.042} Se			1/15 Fe ₇ Se ₈			1/7 Fe ₃ Se ₄		
	(1 mole Fe _{0.510} Se _{0.490} = 67.17 g)			(1 mole Fe _{0.467} Se _{0.533} = 68.18 g)			(1 mole Fe _{0.429} Se _{0.571} = 69.06 g)		
	C _p	S° - S ₀ °	$\frac{H^\circ - H_0^\circ}{T}$	C _p	S° - S ₀ °	$\frac{H^\circ - H_0^\circ}{T}$	C _p	S° - S ₀ °	$\frac{H^\circ - H_0^\circ}{T}$
298.15	27.97	35.300	17.807	29.48	40.920	19.587	31.46	39.974	19.935
300	28.02	35.472	17.843	29.55	41.100	19.648	31.61	40.166	20.006
320	28.55	37.303	18.496	30.40	43.039	20.293	29.12	42.170	20.691
340	29.06	39.048	19.103	31.32	44.908	20.914	28.84	43.921	21.174
360	29.53	40.721	19.669	32.33	46.725	21.521	28.95	45.570	21.602
380	29.95	42.330	20.199	33.48	48.505	22.119	29.17	47.143	21.994
400	30.35	43.878	20.697	34.90	50.259	22.722	29.37	48.646	22.358
420	30.72	45.369	21.165	36.87	52.008	23.346	29.54	50.084	22.696
440	31.07	46.806	21.608	40.27	53.793	24.031	29.69	51.461	23.010
460	31.41	48.194	22.027	34.37	55.582	24.735	29.81	52.783	23.303
480	31.74	49.532	22.425	31.56	56.965	25.066	29.93	54.048	23.577
500	32.05	50.839	22.804	30.93	58.243	25.311	30.03	55.277	23.833
520	32.37	52.100	23.166	30.84	59.451	25.525	30.14	56.455	24.074
540	32.67	53.328	23.512	31.03	60.619	25.724	30.26	57.595	24.301
560	32.98	54.522	23.845	31.42	61.754	25.920	30.39	58.698	24.516
580	33.25	55.681	24.165	32.14	62.872	26.121	30.52	59.764	24.721
600	33.47	56.818	24.472	33.50	63.988	26.343	30.66	60.806	24.916
620	33.67	57.916	24.765	37.04	65.127	26.622	30.82	61.811	25.104
640	33.87	58.989	25.047	56.42	66.635	27.277	31.01	62.793	25.286
660	34.10	60.030	25.318	31.50	67.863	27.667	31.22	63.772	25.462
680	34.37	61.054	25.580	30.86	68.793	27.758	31.52	64.741	25.636
700	34.70	62.056	25.836	30.68	69.685	27.841	31.84	65.691	25.808
720	35.12	63.036	26.088	30.63	70.546	27.919	32.21	66.607	25.981
740	30.07	70.628	32.879	30.61	71.385	27.992	32.61	67.495	26.155
760	29.83	71.427	32.801	30.61	72.203	28.061	33.06	68.372	26.331
780	29.70	72.200	32.723	30.64	73.000	28.126	33.56	69.238	26.509
800	29.69	72.951	32.648	30.70	73.777	28.190	34.11	70.095	26.693
820	29.80	73.684	32.577	30.77	74.534	28.252	34.73	70.943	26.881
840	29.98	74.404	32.513	30.87	75.279	28.313	35.44	71.791	27.076
860	30.26	75.113	32.457	30.98	76.005	28.374	36.28	72.633	27.280
880	30.61	75.812	32.411	31.12	76.720	28.435	37.29	73.479	27.496
900	31.04	76.505	32.376	31.27	77.416	28.496	38.68	74.327	27.728
920	31.55	77.193	32.352	31.45	78.109	28.558	40.86	75.205	27.988
940	32.12	77.878	32.341	31.63	78.784	28.621	44.03	76.111	28.294
960	32.76	78.568	32.339	31.84	79.456	28.686	51.19	77.108	28.681
980	33.47	79.243	32.355	32.07	80.111	28.753	(63)	78.735	29.713
1000	34.22	79.926	32.385	32.33	80.763	28.822	37.17	79.578	29.984
1020	35.03	80.612	32.428	32.63	81.406	28.894	37.58	80.312	30.094
1040	35.85	81.299	32.486	32.94*	82.040	28.968	38.08	81.037	30.245
1050	36.26	81.645	32.520	33.10*	82.359	29.007	38.37	81.400	30.322

* Extrapolated values.

maximum has been observed in the range 5 to 730°K, however, any transitions taking place in $\text{Fe}_{1.04}\text{Se}$ in this region must be of a non-cooperative or Schottky type.

In Fe(II) the degeneracy of the 5 lowest spin states might be removed by the ligand field. The contribution to heat capacity of a changing population on energy levels has been considered by Schottky¹⁵ and is

$$C_s = NkT^{-2} \frac{d^2 \ln \sum g_i \exp(-E_i/kT)}{d(1/T)^2}$$

where N is the number of particles, and g_i the degeneracy of the i th level, separated from the ground state by an energy E_i .

On extrapolating the heat capacity of the high temperature phase downwards, a difference of about $10 \text{ J } ^\circ\text{K}^{-1}$ per mole of iron appears to be present around 600°K. It corresponds closely to the maximum Schottky effect for a two-level system with degeneracy 4 in the upper level and 1 in the lower. In order to test this assumption further the heat capacity contribution of a Schottky effect with $g_1/g_0 = 4$ and $E_1 - E_0 \hat{=} 1360 \text{ cm}^{-1}$ was subtracted from the experimental curve for tetragonal FeSe, see Fig. 3. The resulting non-transitional heat capacity shows a striking similarity to that estimated for Fe_7Se_8 above 200°K, where differences in θ -temperature are of less importance, and supports the view of a non-cooperative magnetic process taking place in tetragonal FeSe.

Above the transformation temperature of the tetragonal PbO-like structure into the hexagonal NiAs-like structure, the heat capacity of $\text{Fe}_{1.04}\text{Se}$ decreases slightly for about 50°K. This decrease might be ascribed to the diminution of short range order in the hexagonal structure above a transition which is obscured by the transformation. The transition is supposedly of cooperative magnetic nature, related to the one in Fe_7Se_8 at 450°K and in Fe_3Se_4 at 307°K.

With further increase in temperature above 800°K the heat capacity of $\text{Fe}_{1.04}\text{Se}$ rises quite rapidly. This might indicate the onset of a new transition or that a disproportionation reaction is taking place in the sample. The latter alternative is in keeping with the observation by Trøften and Kullerud¹⁶ that the maximum melting point (at which the solidus and liquidus curves coincide) for the Fe_{1-x}Se -phase is situated at $1070 \pm 5^\circ\text{C}$ and about 53.0 atomic % Se.

This structural change of the tetragonal FeSe-phase to the hexagonal has been confirmed by high-temperature X-ray data on $\text{FeSe}_{0.92}$; see Table 5

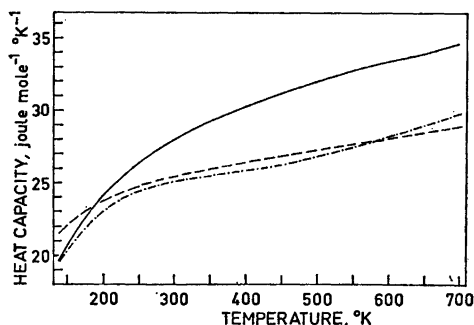


Fig. 3. Subtraction of assumed Schottky heat capacity effect --- ($g_1/g_0 = 4$ and $E_1 - E_0 \hat{=} 1360 \text{ cm}^{-1}$) from experimental data — for tetragonal FeSe. - - represents non-transitional heat capacity of Fe_7Se_8 .

Table 5. Lattice constants, crystal symmetry and unit cell volume for the major phase present in a sample with composition $\text{FeSe}_{0.92}$.

$T, ^\circ\text{C}$	a in Å	c in Å	Symm.	V in Å^3
20	3.771	5.521	tetr.	78.51
105	3.785	5.534	»	79.28
220	3.803	5.553	»	80.31
290	3.809	5.565	»	80.74
390	3.824	5.580	»	81.60
440	3.829	5.585	»	81.88
465	3.753	5.958	hex.	72.68
490	3.756	5.962	»	72.84

and Fig. 4. Both a - and c -axis and the volume increase regularly with temperature for the tetragonal monoselenide up to at least 440°C . In the temperature range between 440 and 465°C the structure changes to hexagonal with about 10 % decrease in volume.

B. Fe_7Se_8 . In Fe_7Se_8 two lambda-type transitions are encountered and it is of interest to attempt a resolution of the heat capacity of the cooperative processes from the other components. A basis of this resolution is found in the usual factoring of the partition function, $Z = \prod Z_i$. The Helmholtz energy $A = -kT \ln Z$ thus involves a sum of $\ln Z_i$ and the thermodynamic functions might accordingly be represented by a sum of contributions from various modes of excitation of the lattice, the unpaired electrons, the conduction electrons *etc.*

The simplest way to approximate the non-cooperative heat capacity of Fe_7Se_8 is by using data for a similar substance with no transitions. When trying to use the measurements¹⁷ on the nickel selenide $\text{Ni}_{0.95}\text{Se}$ for this purpose it turned out that they were too low at low temperatures and too high at the

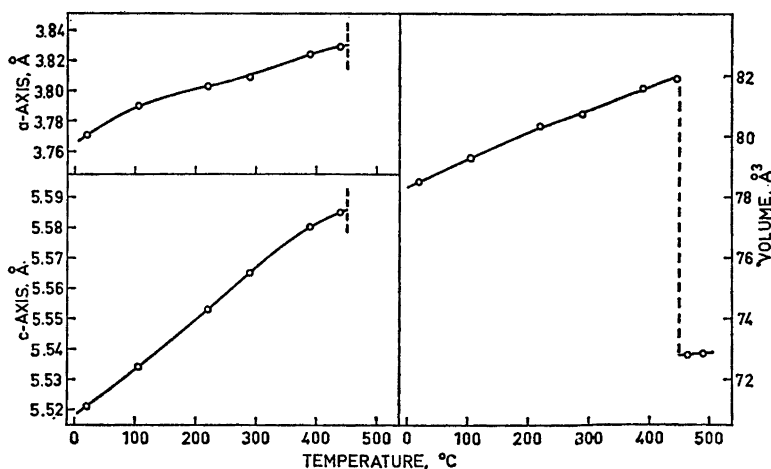


Fig. 4. Lattice constants and unit cell volume for tetragonal FeSe . The cell volume of the hexagonal structure just above the transition is also shown.

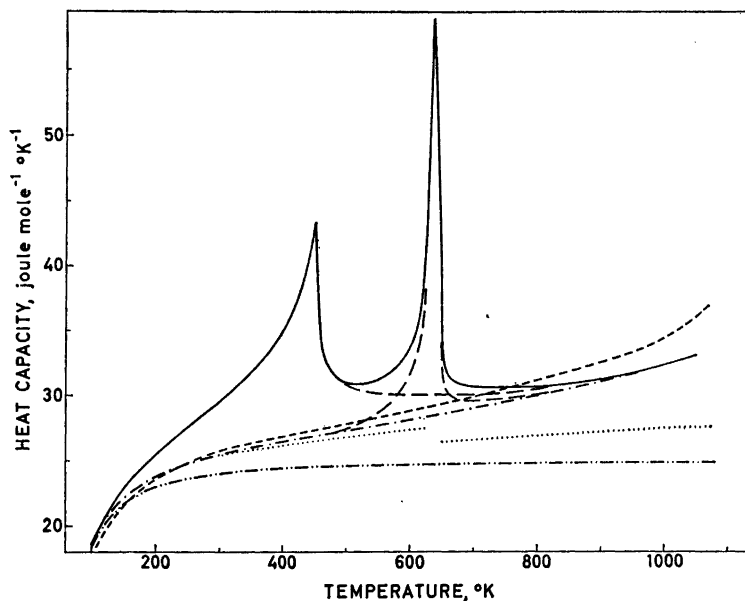


Fig. 5. Attempted resolution of the cooperative processes in Fe_7Se_8 . — represents experimental data, - - - - represents measurements on $\text{Ni}_{0.95}\text{Se}$, - · - · - represents lattice heat capacity at constant volume in the harmonic approximation, · · · · · represents C_v plus Grüneisen dilation contribution, - - - - represents C_v plus adjusted Nernst-Lindemann contribution, and - - - - represents the separated components.

highest temperatures; see Fig. 5. A possible explanation for the deviation at higher temperatures is that the nickel selenide has more metallic character than the iron selenide and thus probably a larger electronic contribution to its heat capacity.

In the absence of detailed knowledge of the vibrational frequency distribution of a substance the heat capacity at constant volume is usually expressed by a Debye function for a monoatomic substance and by a sum of Debye functions, or of Debye and Einstein functions, for a compound:

$$C_v(\text{lattice}) = \sum D(\theta/T) + \sum E(\theta/T)$$

Since heat capacities of solids are measured at constant pressure a dilation correction term, $C_d = C_p - C_v$, has to be added to C_v . The molal dilation correction can be shown to equal

$$C_d = C_p - C_v = (\beta^2/\kappa) V T$$

where β is the volume expansion coefficient, κ the isothermal compressibility, V the molal volume and T the absolute temperature. The equation is of limited use because compressibility data are seldom available. Dilation contributions can, however, be estimated according to Grüneisen¹⁸ as

$$C_d = \beta \Gamma T C_v$$

where $\Gamma = \beta V / (\alpha C_v)$ is the Grüneisen constant. In the zeroth approximation $\Gamma = 2$ and independent of temperature. The values of β for Fe_7Se_8 are derived from lattice constant measurements; see Table 6 and Fig. 6. These data lead

Table 6. Lattice constants and cell volume of Fe_7Se_8 .

$T, ^\circ\text{C}$	a in Å	c in Å	V in Å ³
20	3.617	5.886	66.69
65	3.628	5.875	66.97
105	3.639	5.867	67.28
120	3.643	5.860	67.35
130	3.646	5.852	67.37
165	3.661	5.826	67.62
205	3.668	5.821	67.82
295	3.680	5.829	68.36
340	3.685	5.835	68.62
370	3.694	5.846	69.08
405	3.696	5.852	69.23
495	3.701	5.862	69.54

to a dilation correction which is considerably higher below the structural transition than above it, a result which needs further verification.

In the absence also of expansion data the dilation correction might be estimated according to Nernst and Lindemann¹⁹ as

$$C_d = A' (T/T_i) C_p^2$$

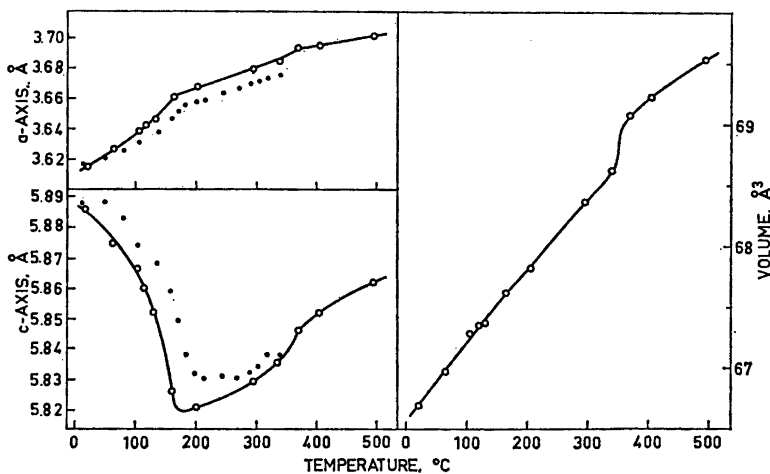


Fig. 6. Lattice constants and cell volume for Fe_7Se_8 in the range 20 to 495°C. O represents present data, ● represents data by Okazaki and Hirakawa.³

where $A' = \beta^2 V T_i / \kappa C_p^2 = 0.0051 \text{ mole } ^\circ\text{K J}^{-1}$ and T_i is the melting temperature of the substance (ideal monoatomic solid). Alternatively the Nernst-Lindemann equation is presented as

$$C_d = AT C_p^2$$

where $A = \beta^2 V / \kappa C_p^2$ varies from substance to substance.

Since the Grüneisen and the Nernst-Lindemann approximations are based of similar arguments the resulting dilation corrections are of the same magnitude, but any abnormal behaviour of the dilation contribution in a transition region escapes the Nernst-Lindemann approximation.

As can be seen from Fig. 5 a large fraction of the increase in heat capacity of Fe_7Se_8 above the classical limit in the high temperature region remains unexplained even though the Nernst-Lindemann approximation often results in an overestimate.²⁰ Since there seems to be no special reason for expecting a rather small compressibility, *i.e.* of the order $\kappa \approx 3.5 \times 10^{-13} \text{ cm}^2 \text{ dyne}^{-1} \approx 3.5 \times 10^{-12} \text{ m}^2 \text{ N}^{-1}$ at 750°K for Fe_7Se_8 , it is concluded that further contributions to the heat capacity are of importance. These contributions might arise from anharmonic lattice vibrations, excited states of the $3d$ -electrons, conduction electrons *etc.*, and warrant further study.

In order to get approximate data for the cooperative processes, the constant A in the Nernst-Lindemann equation and the θ of a single Debye function were used as adjustable parameters to fit the heat capacity data of Fe_7Se_8 at two temperatures far away from the maxima. This approach can, of course, be only moderately successful since spin waves give entropy contributions at low temperatures and the gradual diminution of short range order continues far above the transition. By choosing temperatures of 100 and 1000°K a Debye temperature of 257.5°K and a Nernst-Lindemann constant $A = 7.20 \times 10^{-6} \text{ mole J}^{-1}$ were derived. The resulting curve is shown in Fig. 5. It looks reasonable compared with that of $\text{Ni}_{0.95}\text{Se}$ and has been used for a tentative separation of the peaks from the background. The resulting entropy and enthalpy increments for the two transitions combined are $\Delta S_{\text{tr}} = 7.42 \text{ J } ^\circ\text{K}^{-1}$ and $\Delta H_{\text{tr}} = 3207 \text{ J}$ for $1/15 \text{ mole Fe}_7\text{Se}_8$; see Table 7.

A further separation of these values into their components depends somewhat upon the assumed temperature dependence of the heat capacities in the transition region. In the present case the related structural transition in Ni_7Se_8 was used as a model for the one in Fe_7Se_8 . The transition apparently begins at $T \approx 2/3 T_p$, where T_p is the peak temperature, and is practically completed at $T \approx 4/3 T_p$. By assuming the same reduced shape for the two structural transitions the entropy and enthalpy increments of the magnetic transition (transition I) and the structural transition (transition II) in Fe_7Se_8 were deduced; see Table 7.

For transition I with maximum at 451°K the estimated entropy increment is $13.0 \text{ J } ^\circ\text{K}^{-1}$ per mole of iron atoms. This value is only slightly lower than the spin disorder entropy per mole of iron atoms, assuming $S = 2$ for Fe(II) and $S = 5/2$ for Fe(III):

$$\Delta S = (R/7)(5 \ln 5 + 2 \ln 6) = 13.82 \text{ J mole}^{-1} \text{ } ^\circ\text{K}^{-1}.$$

Table 7. Estimated entropy and enthalpy increments for the transitions in Fe_7Se_8 . Transition I is the ferri- to paramagnetic one with heat capacity maximum at 451°K . Transition II is the structural order-disorder transition with maximum at 638°K . Units: Joule, $^\circ\text{K}$, and $1/15$ mole Fe_7Se_8 .

$T, ^\circ\text{K}$	Total		Trans. I		Trans. II	
	ΔS	ΔH	ΔS	ΔH	ΔS	ΔH
100	0	0	0	0	0	0
140	0.03	5	0.03	5	0	0
160	0.12	18	0.12	18	0	0
180	0.25	38	0.25	38	0	0
200	0.41	68	0.41	68	0	0
220	0.58	106	0.58	106	0	0
240	0.79	152	0.79	152	0	0
260	1.01	208	1.01	208	0	0
280	1.25	274	1.25	274	0	0
300	1.52	351	1.52	351	0	0
320	1.80	439	1.80	439	0	0
340	2.11	541	2.11	541	0	0
360	2.45	659	2.45	659	0	0
380	2.81	793	2.81	793	0	0
400	3.22	949	3.22	949	0	0
420	3.67	1137	3.67	1137	0	0
440	4.21	1371	4.21	1371	0	0
451	4.57	1535	4.57	1535	0	0
460	4.81	1638	4.81	1638	0	0
480	5.05	1751	5.05	1751	0	0
500	5.21	1830	5.21	1829	0	1
520	5.35	1900	5.34	1894	0.01	6
540	5.48	1967	5.44	1951	0.04	16
560	5.60	2037	5.54	2001	0.06	36
580	5.74	2115	5.61	2047	0.13	68
600	5.91	2210	5.68	2088	0.23	122
620	6.12	2346	5.74	2126	0.38	220
638	6.64	2672	5.79	2157	0.85	515
640	6.72	2730	5.80	2160	0.92	570
660	7.08	2963	5.84	2191	1.24	772
680	7.15	3004	5.88	2218	1.27	786
700	7.20	3039	5.92	2242	1.28	797
720	7.24	3071	5.95	2263	1.29	808
740	7.28	3097	5.97	2281	1.31	816
760	7.31	3120	5.99	2297	1.32	823
780	7.34	3139	6.01	2312	1.33	827
800	7.36	3156	6.03	2325	1.33	831
820	7.37	3169	6.04	2337	1.33	832
840	7.39	3180	6.05	2348	1.34	832
860	7.40	3188	6.06	2556	1.34	832
900	7.41	3200	6.07	2568	1.34	832
1000	7.42	3207	6.08	2575	1.34	832

The magnetic moments actually observed by neutron diffraction experiments⁶ are 85 % of the ideal values, and the agreement with the implications of spin disorder is therefore rather satisfactory.

In the earlier work by Hirone and Chiba² the enthalpy of transition I was reported to be 250 cal per mole $\text{FeSe}_{1.13}$, or about 20 % of the value

found here. For the structural transition (transition II) the value shown in Fig. 2 of their paper, 475 cal per mole $\text{FeSe}_{1.13}$, is in reasonable agreement with the present result (426 cal per mole $\text{FeSe}_{1.14}$).

Transition II which takes place in Fe_7Se_8 with maximum at 638°K is obviously connected with the break down of long-range order of the vacancies. The room temperature structure of the calorimetric sample is hexagonal with $A = 2a$ and $C = 3c$, while at 400°C the doubling and tripling have disappeared.* Since there are no changes in the crystallographic unit cell at the ferri- to paramagnetic transition according to Okazaki,⁵ the crystallographic change is assumed to be exclusively connected with transition II. In the ordered structure of Fe_7Se_8 there are planes of iron atoms parallel to the c -axis. Every other of these planes is completely occupied by iron atoms, while in the rest one iron atom out of four is missing.

Assuming now that the order-disorder process involves the partly filled layers only, the resulting disorder entropy is in the zeroth approximation

$$\Delta S = -(\text{R}/2)(0.25 \ln 0.25 + 0.75 \ln 0.75) = 2.34 \text{ J }^\circ\text{K}^{-1}$$

per 0.875 mole of iron atoms. Another alternative is that the distribution of vacancies and iron atoms becomes random and thus equal on both sets of planes, which results in a disorder entropy of

$$\Delta S = -\text{R}(0.125 \ln 0.125 + 0.875 \ln 0.875) = 3.13 \text{ J }^\circ\text{K}^{-1}$$

per 0.875 mole of iron atoms.

Finally, if the disorder involves vacancies and distinguishable iron atoms Fe(II) and Fe(III) the resulting molal entropy increase is

$$\begin{aligned} \Delta S &= -\text{R}(0.125 \ln 0.125 + 0.25 \ln 0.25 + 0.625 \ln 0.625) \\ &= 7.48 \text{ J }^\circ\text{K}^{-1} \end{aligned}$$

The assumption of disorder only within partly filled iron layers agrees best with the experimentally determined entropy increment. It is also in keeping with the observation by Okazaki of the presence of 001, 003 *etc.* reflections in the X-ray photographs of Fe_7Se_8 up to 375°C. Okazaki states that the distribution of vacancies becomes completely disordered around 400°C, but the heat capacity data fail to reveal any further transition in this region.

C. Fe_3Se_4 . In Fe_3Se_4 a ferri- to paramagnetic transition occurs with maximum at 307°K. After fitting a smooth curve to the heat capacity data at 200 and 350°K the entropy increment of the transition was estimated¹ to be $\Delta S = 8 \text{ J }^\circ\text{K}^{-1}$ per mole Fe_3Se_4 . This increment is less than one fifth of the expected value for the spin-disorder process, $\Delta S = (\text{R}/3)(\ln 5 + 2 \ln 6) = 14.4 \text{ J }^\circ\text{K}^{-1}$ per mole of iron atoms, assuming $S = 2$ for Fe(II) and $S = 5/2$ for Fe(III). Thus, the number of spin states available to the 3*d*-electrons might be smaller, or the transition might be of a less cooperative nature and spread over a larger temperature interval.

* The presence of both the 3*c*- and 4*c*-structure types in Fe_7Se_8 has been reaffirmed in recent neutron diffraction work by Kawaminami and Okazaki (*J. Phys. Soc. Japan* 22 (1967) 924). Possibly, the 4*c*-structure contains a little more iron than the 3*c*-structure and has therefore not been observed in the present study.

As a result of extending the heat capacity measurements on Fe_3Se_4 to high temperatures, the unusually high values above the ferri- to paramagnetic transition became evident. Accordingly, the non-transitional heat capacity estimated for 1/15 mole Fe_7Se_8 is 2–3 $\text{J}^\circ\text{K}^{-1}$ lower than the heat capacity of 1/7 mole Fe_3Se_4 over the whole range 350 to 750°K. The high heat capacity in this region is probably not caused by a phase reaction taking place in the sample, since neither the uptake of any unreacted selenium causing a decrease in heat capacity, nor the peritectic decomposition¹⁶ of any FeSe_2 at 585°C were detected.

An attempt to reevaluate the entropy increment of transition in Fe_3Se_4 without neglecting contributions of less cooperative nature was therefore made using the same background as for Fe_7Se_8 . It appeared then that the transitional entropy acquired from 100°K to the Curie point at 304°K amounts to only 2.3 $\text{J}^\circ\text{K}^{-1}$ for one mole of iron atoms. This should correspond to between 73 and 90 % of the total for a Heisenberg and Ising model fcc ferromagnet²¹ with $S = \frac{1}{2}$, or 80 % of the total by comparing it with Fe_7Se_8 (cf. Table 7). Thus, it appears just as for the chromium tellurides²² that the entropy acquired in the cooperative disorder process is only a fraction of the expected value. In Fe_3Se_4 the remaining disorder entropy is probably acquired in a non-cooperative, or Schottky-type, process with maximum in the range 400 to 600°K. In the absence of any details about the splittings and degeneracies of the 3d energy levels a simple assumption is that the process involves one doubly and one triply degenerate level in case of Fe(II) and one doubly and one quadruply degenerate level in case of Fe(III). If the Schottky heat capacities are assumed to have their maxima at 450°K, corresponding to $\Delta E \cong 780 \text{ cm}^{-1}$ for Fe(II) and $\Delta E \cong 830 \text{ cm}^{-1}$ for Fe(III), the composite maximum should amount to 2.53 $\text{J}^\circ\text{K}^{-1}$ for 1/7 mole Fe_3Se_4 . The attempted resolution is shown in Fig. 7 after a slight adjustment of the dilation contribution, taking $\theta = 275^\circ\text{K}$ and $A = 0.0104 \text{ mole J}^{-1}$. It is seen to explain the observed discrepancy rather well and leads to a total entropy increment for the magnetic transition of 10.5 $\text{J}^\circ\text{K}^{-1}$ per mole of iron atoms. The value is 73 % of the expected one and might indicate that the dilation contribution has been overestimated.

The presented picture of a superimposed cooperative and non-cooperative process being responsible for the magnetic transition in Fe_3Se_4 needs further

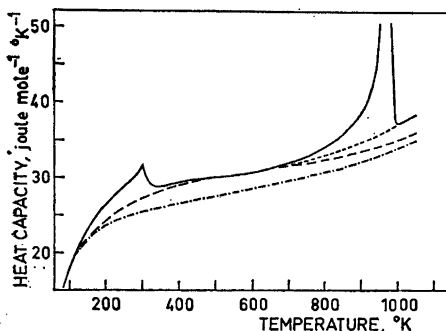


Fig. 7. Attempted resolution of the cooperative processes in Fe_3Se_4 . — represents experimental data, --- represents C_v plus adjusted Nernst-Lindemann contribution, - - represents C_v plus Nernst-Lindemann plus assumed Schottky contribution, . . represents alternative background for the 977°K peak.

verification and correlation with other data. Although the interatomic distances in Fe_3Se_4 are not known in detail, the shortest iron-iron distances should be about 2.85 Å, or 0.10 Å shorter than in Fe_7Se_8 due to the lattice contraction with increasing selenium content. Accordingly, the low magnetic moment of 0.2 μB per iron atom²³ might be taken as an indication of the more collective nature of its 3*d*-electrons. Recent neutron diffraction work²⁴ indicates that the spins in the ferrimagnetic structure are only $S=1.08$ for Fe(II) and $S=0.71$ for Fe(III). The corresponding disorder entropy $\Delta S = 8.08 \text{ J } ^\circ\text{K}^{-1}$ is, however, somewhat lower than that deduced from the experimental data.

The second λ -type transition in Fe_3Se_4 has its maximum at 977°K. Estimates of the associated heat capacity, entropy and enthalpy increments have been made after adding the tail of the assumed Schottky effect to the non-transitional heat capacity. Above the maximum the transition is obscured to some extent by the exsolution of selenium from the Fe_3Se_4 -phase. In the absence of any quantitative data, this effect is assumed to be balanced by considering the transition to be complete at 1000°K. The resulting entropy and enthalpy increments are $\Delta S = 3.98 \text{ J } ^\circ\text{K}^{-1}$ and $\Delta H = 3570 \text{ J}$ per mole $\text{Fe}_{0.75}\text{Se}$. A more conservative estimate was made by joining a smooth curve to the experimental data at 650 and 1000°K; see Fig. 7. It results in the somewhat lower values $\Delta S = 3.05 \text{ J } ^\circ\text{K}^{-1}$ and $\Delta H = 2920 \text{ J}$ per mole $\text{Fe}_{0.75}\text{Se}$. The entropy of transition is presently taken as $\Delta S = 3.5 \pm 0.5 \text{ J } ^\circ\text{K}^{-1}$ per mole $\text{Fe}_{0.75}\text{Se}$.

The nature of this transition is probably structural and connected with disordering of vacancies and raising of the symmetry of the structure from monoclinic to hexagonal on heating. Just as for Fe_7Se_8 the entropy increment can be compared with those calculated for 0.75 mole of iron atoms assuming:

- a) Disorder of vacancies within half filled iron planes,
 $\Delta S = -R(0.5 \ln 0.5) = 2.88 \text{ J } ^\circ\text{K}^{-1}$,
- b) Disorder of vacancies on all iron positions,
 $\Delta S = -R(0.25 \ln 0.25 + 0.75 \ln 0.75) = 4.67 \text{ J } ^\circ\text{K}^{-1}$,
- c) Disorder of vacancies, Fe(II) and Fe(III) on all iron positions,
 $\Delta S = -R(0.5 \ln 0.25 + 0.5 \ln 0.5) = 8.64 \text{ J } ^\circ\text{K}^{-1}$.

Again the assumption of disorder within every other layer corresponds best to the observations. The result is seen as a confirmation of the early view by Tengnér²⁵ and Hoschek and Klemm²⁶ that in the transition from the NiAs-type to the $\text{Cd}(\text{OH})_2$ -type structure vacant positions are created only in every other metal layer in the *ab*-plane.

Acknowledgements. The continued financial support by *Norges Almenvitenskapelige Forskningsråd* is gratefully acknowledged. The assistance of Nils Erik Askheim, Karin Bjåmer, Andreas Bugge, Jens Erik Bøe, Inge Fjerdningstad, Anders Langen, Bjørn Lyng-Nilsen, Eivind Sætre, Jan Thorstensen and Leiv Egil Vestersjø in various phases of the time-consuming measurements and calculations is thankfully recognized. Results obtained using two earlier versions of the calorimeter are superseded by the present. The assistance of Torkild Thurmann-Moe, Grete Bendtsen and Tor Tufte during those stages of the work was of no less importance and is also recognized with thanks. The selenium used was generously supplied by Bolidens Gruvaktiebolag.

REFERENCES

1. Grønvold, F. and Westrum, E. F., Jr. *Acta Chem. Scand.* **13** (1959) 241.
2. Hirone, T. and Chiba, S. *J. Phys. Soc. Japan* **11** (1956) 666.
3. Okazaki, A. and Hirakawa, K. *J. Phys. Soc. Japan* **11** (1956) 930.
4. Okazaki, A. *J. Phys. Soc. Japan* **14** (1959) 112.
5. Okazaki, A. *J. Phys. Soc. Japan* **16** (1961) 1162.
6. Andresen, A. F. and Leciejewicz, J. *J. Phys. Radium* **25** (1964) 574.
7. Hägg, G. and Kindström, A.-L. *Z. physik. Chem.* **B 22** (1933) 453.
8. Grønvold, F. *Acta Chem. Scand.* **21** (1967) 1695.
9. Hambling, P. G. *Acta Cryst.* **6** (1953) 98.
10. Svendsen, S. R. *Personal communication*.
11. Hoge, H. J. *J. Res. Natl. Bur. Std.* **36** (1946) 111.
12. Reshetnikov, M. A. *Izv. Sektora Fiz. Khim. Analiza, Inst. Obshch. Neorg. Khim. Akad. Nauk SSSR* **23** (1953) 9; according to Shmidt, N. E. and Sokolov, V. A. *Russ. J. Inorg. Chem.* **5** (1960) 797.
13. Hirone, T., Maeda, S. and Tsuya, N. *J. Phys. Soc. Japan* **9** (1954) 496.
14. Haraldsen, H. and Grønvold, F. *Tidsskr. Kjemi, Bergvesen, Met.* **10** (1944) 98, Structure Reports **9** (1955) 97, and unpubl. results.
15. Schottky, W. *Phys. Z.* **23** (1922) 448.
16. Trøften, P. and Kullerud, G. *Carnegie Inst. Wash. Year Book* **60** (1961) 176.
17. Grønvold, F. *Unpublished results*.
18. Grüneisen, E. *Ann. Physik* **26** (1908) 393; **39** (1912) 257; See also *Handbuch der Physik* **10** (1926) 1.
19. Nernst, W. and Lindemann, F. A. *Z. Elektrochem.* **17** (1911) 817.
20. Chang, Y. A. and Hultgren, R. *J. Phys. Chem.* **69** (1965) 4162.
21. Domb, C. and Sykes, M. F. *Phys. Rev.* **128** (1962) 168.
22. Grønvold, F. and Westrum, E. F., Jr. *Z. anorg. allgem. Chem.* **328** (1964) 272.
23. Hirakawa, K. *J. Phys. Soc. Japan* **12** (1957) 929.
24. Andresen, A. *Acta Chem. Scand.* **22** (1968) 827.
25. Tengnér, S. *Z. anorg. allgem. Chem.* **239** (1938) 126.
26. Hoschek, E. and Klemm, W. *Z. anorg. allgem. Chem.* **242** (1939) 49.

Received October 7, 1967.